JOM, Vol. 72, No. 6, 2020
https://doi.org/10.1007/s11837-020-04083-x

Modeling the Effects of Filler Network and Interfacial Shear Strength on the Mechanical Properties of Carbon Nanotube-Reinforced Nanocomposites

YASSER ZARE [1] and KYONG YOP RHEE [1,2]

1.—Department of Mechanical Engineering, College of Engineering, Kyung Hee University, 1 Seocheon, Giheung, Yongin, Gyeonggi 449-701, Republic of Korea. 2.—e-mail: rheeky@khu.ac.kr

This modeling paper describes the roles of filler network and imperfect interfacial adhesion between polymer matrix and nanoparticles in the tensile modulus and yield strength of polymer/carbon nanotube (CNT) nanocomposites (PCNT). The percolation threshold (ϕ_p) is assumed by the aspect ratio of the CNT; also, both the critical length of the nanotubes. Crucial for effective stress transfer from matrix to filler (L_c). and the interfacial shear strength (τ) reflect the incomplete interfacial adhesion. Two known micromechanics models are used to examine the influences of these parameters on the tensile modulus and yield strength of PCNT. The lowest ranges of ϕ_p and L_c produce the highest levels of mechanical properties, while τ cannot affect the mechanical performance. The main reasons for these occurrences are explained in order to clarify the roles of the filler network and interfacial adhesion in the modulus and strength of PCNT.

INTRODUCTION

A low content of carbon nanotubes (CNT)[1–8] or graphene[9–18] can make a polymer nanocomposite with significant stiffness, strength, heat distortion temperature (HDT) and barrier properties. The high levels of aspect ratio, specific surface area and stiffness of these nanoparticles are responsible for the substantial properties. The anti-static, electromagnetic shielding and electrical conductivity of polymer/CNT nanocomposites (PCNT) result in applications in biomedical devices, and in electronics, automotive and aerospace industries.[19–24] The PCNT are electrically conductive materials showing many benefits over conventional composites, such as noble thermal and mechanical performance, high electrical conductivity and low viscosity, allowing them to be simply molded at very low fractions of CNT. However, PCNT suffer from some problems, such as poor dispersion and waviness of the nanoparticles, which have motivate researchers to solve these deficiencies.[25–27]

The general properties of polymer/CNT nanocomposites (PCNT) depend on many factors, such as the concentration, aspect ratio, strength and dispersion superiority of CNT, as well as the interphase properties between the polymer matrix and the CNT.[28–31] The interphase around the nanoparticles generally determines the molecular interaction at the nanoscale, which demonstrates the efficiency of the stress transfer from the polymer to the nanoparticles. Accordingly, a poor interphase eliminates the main advantages of nanoparticles in nanocomposites, such as excellent stiffness. However, the nanoscale manipulation limits the experimental measurement of the interphase dimension and strength. For this reason, theoretical models have been used to investigate the interphase characteristics. Previous studies found that the interphase with significant thickness and strength extensively controls the mechanical performance of nanocomposites.[32–35] An inadequate interfacial adhesion is commonly formed in many PCNT, which makes for a weak stress transfer from the polymer matrix to the nanoparticles. This occurrence is attributed to the incompatibility or lower compatibility between the polymer and the nanoparticles, as well as the aggregation/agglomeration and poor dispersion of the nanofiller or non-fitting processing parameters.[36–39] In nanocomposites, the main issue is the

 (Published online March 3, 2020)

agglomeration of nanoparticles (hard layers) in the case of a lubricating matrix. Protective coatings for tribological applications fundamentally require the proper levels of hardness, toughness, and interfacial adhesion with the underlying substrate.[40] To enhance the mechanical properties of these nanocoatings, the importance of these terms should be considered. The dispersion quality of nanoparticles affects the toughness, but the hardness, as the resistance to localized plastic deformation encouraged by mechanical indentation or abrasion, depends on many parameters, such as the elastic stiffness, strength, toughness, viscoelasticity, and shear modulus.

In this article, we focus on the interfacial adhesion between the polymer matrix and the nanoparticles, which mainly governs the tensile modulus and yield strength of nanocomposites, because the interface properties control the stress transferring from the matrix to the filler. Moreover, an adhesive interfacial layer between the substrate and crystalline/amorphous coating is essential for reducing the wear rate, which serves the dual purpose of enhancing the adhesion and stress relief.[41] Laser cladding and laser annealing are also utilized to melt the materials, which can lead to a tremendous improvement in the adhesion of the coating materials.[42]

On the other hand, the formation of a connected network of nanotubes above the percolation threshold has been reported in PCNT.[43,44] The percolation threshold is the smallest volume fraction of the nanoparticles, which form a continuous network in the polymer matrix.[45,46] The percolation threshold meaningfully raises the electrical conductivity of the nanocomposite, which changes the insulating polymer matrix to a conductive sample. The percolation threshold is also effective for the mechanical properties of polymer nanocomposites.[47,48] Favier et al.[47] reported the high shear modulus of reinforced films with cellulose whiskers by percolation. Many theoretical approaches have been applied to consider and predict the effect of the percolation threshold on the mechanical behavior of polymer nanocomposites. The micromechanics models assessed the deformation energy stored in the tubes to determine the modulus.[49,50] Chatterjee[51] combined the Halpin–Tsai model assuming dispersed particles with the results from the networked filler and presented a model for the modulus of nanocomposites containing dispersed and networked nanofillers. However, this model needs some adjustable parameters for modeling, which is incorrect. Generally, the percolation threshold in the mechanical performances of polymer nanocomposite has been only briefly studied in the literature.

In this study, the percolation threshold (ϕ_p) in PCNT is assumed by the aspect ratio of the CNT. Also, the incomplete interfacial adhesion is considered by the average normal stress, which suggests the effective aspect ratio and volume fraction of the CNT. After that, two known micromechanics models have been applied to study the effects of ϕ_p and effective parameters on the tensile modulus and yield strength of the PCNT. The present paper reports that the levels of ϕ_p and the interfacial adhesion have significant roles in the mechanical performances of PCNT.

Nomenclature

σ_f: tensile strength of CNTs, σ: normal stress, L_c: critical length of CNT essential for effective stress transferring, D: CNT diameter, l: CNT length, α: inverse aspect ratio, τ: interfacial shear strength, α_{eff}: effective CNT aspect ratio, ϕ_{eff}: effective CNT volume fraction, ϕ_f: CNT volume fraction, ϕ_p: percolation threshold, E_c: Young's modulus of nanocomposite, E_m: matrix modulus, E_f: CNT modulus, σ_c: yield strength of nanocomposite, σ_m: strength of polymer matrix, s: interfacial stress transfer parameter.

THEORETICAL VIEWS

A poor interfacial adhesion cannot bear the high interfacial shear stress during stress loading, which causes yielding or debonding at or near the interface. In this condition, the interfacial shear stress presents a low build-up of normal stress in the tube and a large distance is essential for normal stress to reach the tensile strength of the tubes (σ_f).[52] As a result, a large portion of the tubes is not completely loaded due to imperfect interfacial adhesion, which decreases the strengthening effect of the nanoparticles.

Figure 1 shows the profiles of normal stress (σ) in a tube in two states. In the first case ($L_c \le x \le l/2$), σ reaches σ_f before the full length of the tube debonds. However, the complete length of the tube is involved before reaching σ to σ_f when $0 \le x \le L_c$. In the second case. L_c is the critical length of the tube, which is essential for the effective transfer of stress from the matrix to the tube, i.e. L_c is the crucial distance for σ to reach σ_f.

L_c is expressed as:

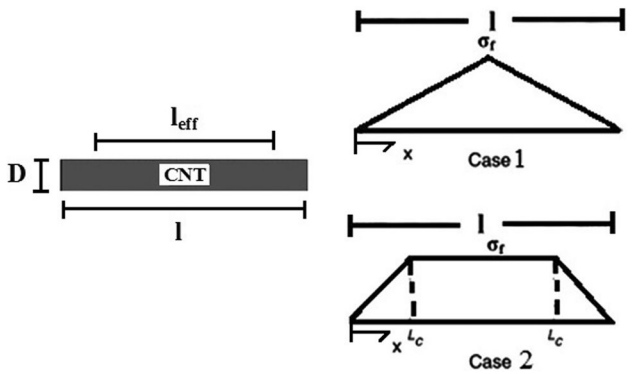

Fig. 1. The effective length of a tube (l_{ef}) assuming incomplete interfacial adhesion and the profiles of normal stress at two different cases of (1) $x < 2L_c$ and (2) $x > 2L_c$

$$L_c = \frac{\sigma_f D}{2\tau} = \frac{\sigma_f \alpha l}{2\tau} \quad (1)$$

where D and l are the diameter and length of the tube, respectively and α is the inverse aspect ratio, as $\alpha = D/l$. Also, τ is the interfacial shear strength.

The average normal stress ($\bar{\sigma}$) equals σ_f when a tube is perfectly adhered to the matrix, but $\bar{\sigma}$ is less than σ_f in the case of incomplete interfacial adhesion, which results in a smaller effective length of the tube than l[52] as:

$$\bar{\sigma} l = \sigma_f l_{eff} \quad (2)$$

As a result, the effective aspect ratio (α_{eff}) and volume fraction (ϕ_{eff}) of nanotubes are reduced by poor interfacial bonding, which decreases their reinforcing efficiency in PCNT.

α_{eff} and ϕ_{eff} in the case of $l < 2L_c$ (case 1) were defined[52] as:

$$\alpha_{eff} = \alpha \frac{4L_c}{l} \quad (3)$$

$$\phi_{eff} = \phi_f \left(\frac{l}{4L_c} \right) \quad (4)$$

where ϕ_f is the volume fraction of the nanofiller in the sample. Moreover, when $l > 2L_c$ (case 2), it was stated[52] that:

$$\alpha_{eff} = \alpha \left(\frac{1}{1 - \frac{L_c}{l}} \right) \quad (5)$$

$$\phi_{eff} = \phi_f \left(1 - \frac{L_c}{l} \right) \quad (6)$$

Assuming that the tubes comprise $x < 2L_c$ and $x > 2L_c$ region (Fig. 1), α_{eff} and ϕ_{eff} parameters are expressed for the tubes as:

$$\alpha_{eff} = \frac{2L_c}{l} \left(\alpha \frac{4L_c}{l} \right) + \left(\frac{l - 2L_c}{l} \right) \alpha \left(\frac{1}{1 - \frac{L_c}{l}} \right) = \alpha \left(\frac{8L_c^2}{l^2} + 1 \right) \quad (7)$$

$$\phi_{eff} = \frac{2L_c}{l} \left(\phi_f \frac{l}{4L_c} \right) + \left(\frac{l - 2L_c}{l} \right) \phi_f \left(1 - \frac{L_c}{l} \right) = \phi_f \left[\frac{1}{2} + \left(\frac{l - 2L_c}{l^2} \right) (l - L_c) \right] \quad (8)$$

When L_c is replaced from Eq. 1 into Eqs. 7 and 8, the effective factors are suggested as:

$$\alpha_{eff} = \alpha \left(\frac{2\sigma_f^2 \alpha^2}{\tau^2} + 1 \right) \quad (9)$$

$$\phi_{eff} = \phi \left[\frac{1}{2} + \left(1 - \frac{\sigma_f \alpha}{\tau} \right) \left(1 - \frac{\sigma_f \alpha}{2\tau} \right) \right] \quad (10)$$

Chatterjee[51] suggested an opposite linking between the volume fraction of the geometric percolation threshold (ϕ_p) and the inverse aspect ratio of CNT (α) as:

$$\phi_p \approx \alpha \quad (11)$$

Using the above equation, the effective parameters in Eqs. 7–10 can be expressed by ϕ_p, L_c and τ as:

$$\alpha_{eff} = \phi_p \left(\frac{8L_c^2}{l^2} + 1 \right) \quad (12)$$

$$\alpha_{eff} = \phi_p \left(\frac{2\sigma_f^2 \phi_p^2}{\tau^2} + 1 \right) \quad (13)$$

$$\phi_{eff} = \phi_f \left[\frac{1}{2} + \left(1 - \frac{\sigma_f \phi_p}{\tau} \right) \left(1 - \frac{\sigma_f \phi_p}{2\tau} \right) \right] \quad (14)$$

To evaluate the effects of the ϕ_p, L_c and τ parameters on the tensile modulus and yield strength of P the CNT, two known micromechanics models are applied.

The Halpin–Tsai model[53] is widely used for the calculation of the tensile modulus in PCNT, which is given by:

$$E_R = \frac{1 + 2\eta\phi_f/\alpha}{1 - \eta\phi_f} \quad (15)$$

$$\eta = (E_f/E_m - 1)/(E_f/E_m + 2/\alpha) \quad (16)$$

where $E_R = E_c/E_m$, and E_c, E_m and E_f are the Young's moduli of the nanocomposite, the polymer matrix and the nanoparticles, respectively. Inserting the effective parameters into the Halpin–Tsai model results in:

$$E_R = \frac{1 + \frac{2\eta\phi_f \left[\frac{1}{2} + \left(\frac{l - 2L_c}{l^2} \right) (l - L_c) \right]}{\phi_p \left(\frac{8L_c^2}{l^2} + 1 \right)}}{1 - \eta\phi_f \left[\frac{1}{2} + \left(\frac{l - 2L_c}{l^2} \right) (l - L_c) \right]} \quad (17)$$

$$\eta = (E_f/E_m - 1)/\left[E_f/E_m + \frac{2}{\phi_p \left(\frac{8L_c^2}{l^2} + 1 \right)} \right] \quad (18)$$

Moreover, the Halpin–Tsai model can be presented as a function of ϕ_p and τ by the effective parameters as:

$$E_R = \frac{1 + \frac{2\eta\phi_f\left[\frac{1}{2}+\left(1-\frac{\sigma_f\phi_p}{\tau}\right)\left(1-\frac{\sigma_f\phi_p}{2\tau}\right)\right]}{\phi_p\left(\frac{2\sigma_f^2\phi_p^2}{\tau^2}+1\right)}}{1-\eta\phi_f\left[\frac{1}{2}+\left(1-\frac{\sigma_f\phi_p}{\tau}\right)\left(1-\frac{\sigma_f\phi_p}{2\tau}\right)\right]} \quad (19)$$

$$\eta = (E_f/E_m - 1)/\left[E_f/E_m + \frac{2}{\phi_p\left(\frac{2\sigma_f^2\phi_p^2}{\tau^2}+1\right)}\right] \quad (20)$$

Additionally, the dependence of the yield strength of the PCNT to the material and interfacial properties can be displayed by the Callister model[54] as:

$$\sigma_R = 1 + \left(\frac{s}{\alpha\sigma_m} - 1\right)\phi_f \quad (21)$$

where σ_R is the relative yield strength as $\sigma_R = \sigma_c/\sigma_m$, and σ_c and σ_m are the yield strengths of the nanocomposite and the polymer matrix, respectively. Also, s is an interfacial stress transfer parameter, which demonstrates the quality of interfacial adhesion. Substituting the effective parameters in this model results in:

$$\sigma_R = 1 + \left[\frac{s}{\phi_p\left(\frac{8L_c^2}{l^2}+1\right)\sigma_m} - 1\right]\left[\frac{1}{2}+\left(\frac{l-2L_c}{l^2}\right)(l-L_c)\right]\phi_f \quad (22)$$

Also, the Callister model (Eq. 21) can be presented by the ϕ_p and τ parameters by replacing the effective parameters as:

$$\sigma_R = 1 + \left[\frac{s}{\phi_p\left(\frac{2\phi_p^2\phi_f^2}{\tau^2}+1\right)\sigma_m} - 1\right] \times \left[\frac{1}{2}+\left(1-\frac{\phi_p\sigma_f}{\tau}\right)\left(1-\frac{\phi_p\sigma_f}{2\tau}\right)\right]\phi_f \quad (23)$$

RESULTS AND DISCUSSION

In this section, the micromechanics models are used to investigate the effects of the percolation threshold by ϕ_p and the effective parameters (α_{eff} and ϕ_{eff}) by L_c and τ on the tensile modulus and yield strength of the PCNT. The software utilized to perform the simulations is MATLAB.

Figure 2 illustrates the 3D and contour plots of E_R as a function of the ϕ_p and L_c parameters according to Eqs. 17 and 18 at average values of ϕ_f = 0.02, l = 5 μm, E_m = 3 GPa and E_f = 1000 GPa. The worst modulus is observed at the highest levels of the ϕ_p and L_c parameters. Also, the highest modulus is achieved by the smallest ranges of these parameters. Therefore, the values of the ϕ_p and L_c parameters inversely affect the tensile modulus of the PCNT. The ϕ_p parameter determines the volume fraction of nanoparticles in which the CNT forms a network. Clearly, a low value of ϕ_p shows the formation of a CNT network in the polymer matrix at a low volume fraction of nanoparticles. In this status, the PCNT contains a network of CNT with a low fraction of nanoparticles, which reinforces the polymer matrix, well. As a result, a small level of ϕ_p makes a stiff PCNT by the low concentration of CNT, and the higher levels of ϕ_f strengthens the CNT network more. On the other hand, the L_c parameter shows the surface fraction of the nanotubes, which can effectively bear the load due to complete interfacial adhesion.

As explained, a low L_c indicates the great efficiency of stress transfer between the polymer matrix and the nanoparticles, because $\bar{\sigma}$ reaches the σ_f at $x > 2L_c$. However, a higher level of L_c shows the larger area of tubes, which poorly transfers the load from the matrix to the tubes and weakens the modulus. Accordingly, E_R shows a reasonable relationship with the ϕ_p and L_c parameters based on the Halpin–Tsai model.

Figure 3 displays the roles of the ϕ_p and τ parameters on the tensile modulus of the PCNT according to the Halpin–Tsai model (Eqs. 19 and 20) at ϕ_f = 0.02, E_m = 3 GPa, E_f = 1000 GPa and σ_f = 1.7 GPa. It is obvious that the ϕ_p parameter plays the main role in the modulus of the PCNT, while the τ factor cannot change the modulus in this condition. Also, an E_R value of about 5 is observed at ϕ_p = 0.01, while E_R = 8.5 is achieved by ϕ_p = 0.001. Both the upper and lower levels of E_R are calculated at the different levels of τ, demonstrating the ineffective role of τ in the modulus. Accordingly, the modulus mainly depends on the ϕ_p parameter and τ does not play a role. Moreover, an inverse relationship is observed between the modulus and the ϕ_p parameter, where the highest modulus is observed at the lowest level of ϕ_p. This trend is reasonable, due to the network formation in the PCNT at ϕ_p. A low level of ϕ_p shows the formation of the network by the low fraction of CNT, which induces a strong sample at different levels of CNT concentration. In addition, the ineffective role of τ as the interfacial shear strength between the polymer matrix and the nanoparticles may be due to the high level of E_f of 1000 GPa and low level of σ_f of 1.7 GPa. The roles of the τ parameter in the modulus and the strength of the polymer nanocomposites have been shown in previous articles,[55,56] but its character may be eliminated when it is compared with ϕ_p as a main parameter, which shows the networking of the CNT in the polymer nanocomposites. A CNT network can endure a high capacity of load and, thus, it can considerably reinforce the polymer matrix.

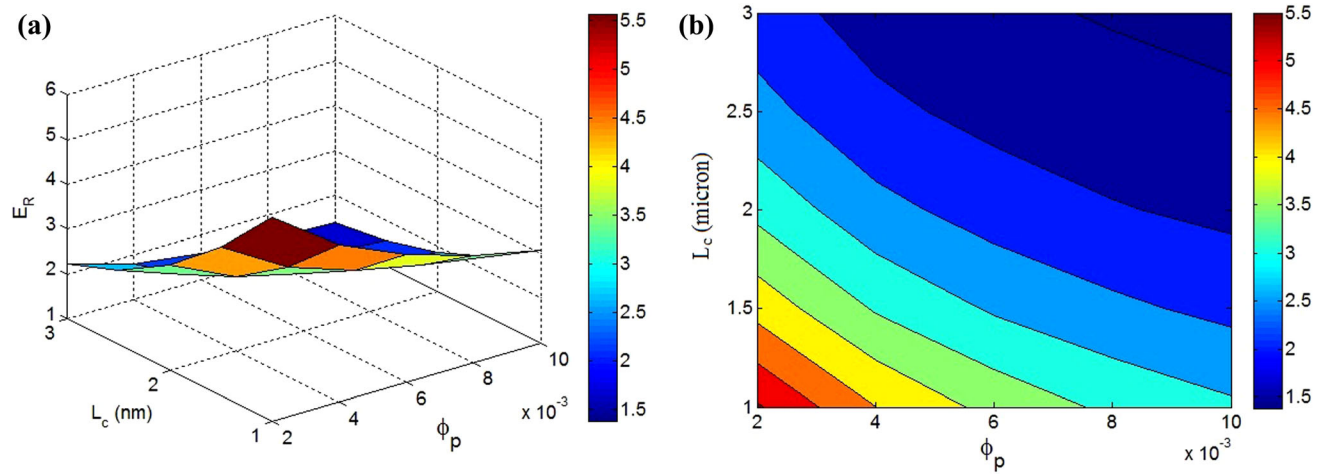

Fig. 2. (a) 3D and (b) contour plots to show E_R as a function of ϕ_p and L_c parameters by Eqs. 17 and 18 at average values of ϕ_f = 0.02, l = 5 μ, E_m = 3 GPa and E_f = 1000 GPa

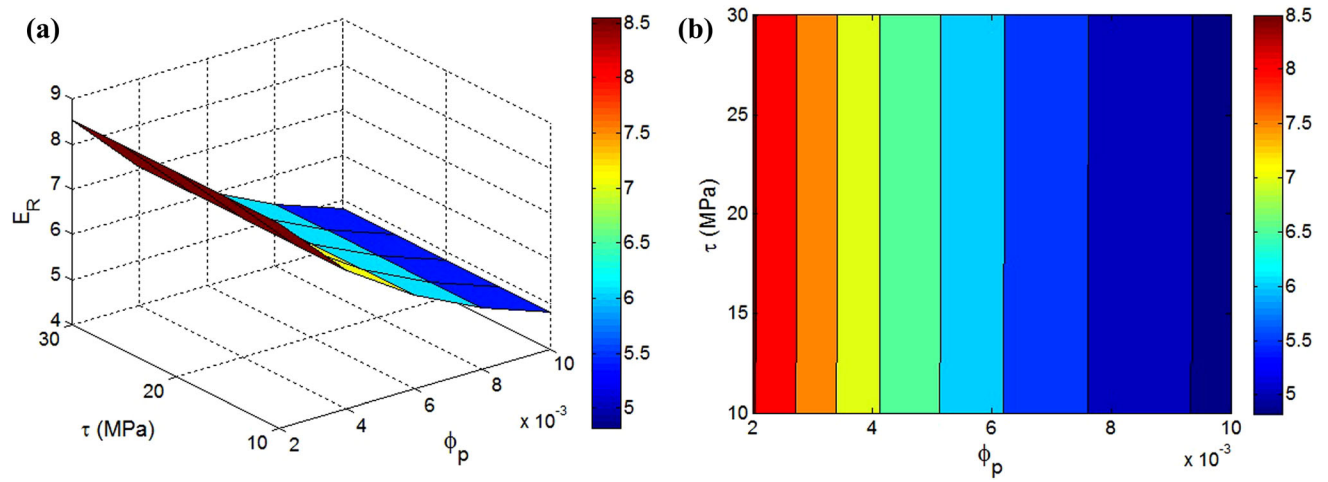

Fig. 3. The effects of ϕ_p and τ parameters on E_R according to the Halpin–Tsai model (Eqs. 19 and 20) at ϕ_f = 0.02, E_m = 3 GPa, E_f = 1000 GPa and σ_f = 1.7 GPa: (a) 3D and (b) contour plots

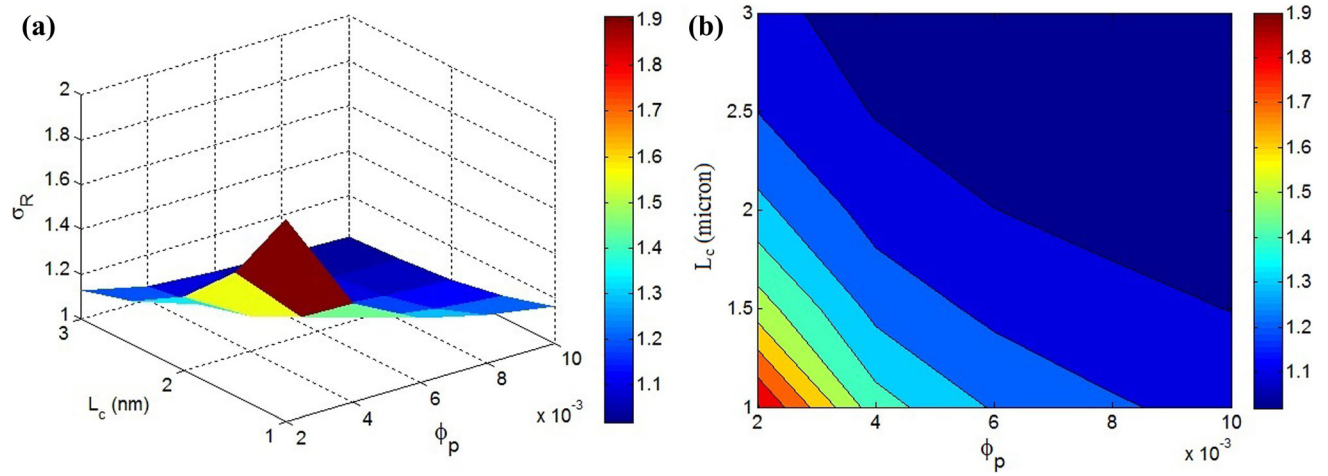

Fig. 4. (a) 3D and (b) contour plots of σ_R as a function of ϕ_p and L_c parameters according to Eq. 22 at average values of ϕ_f = 0.02, σ_m = 40 MPa, l = 5 μ and s = 5 MPa

Figure 4 shows the influences of the ϕ_p and L_c parameters on σ_R according to the Callister model (Eq. 22) at average values of $\phi_f = 0.02$, $\sigma_m = 40$ MPa, $l = 5$ μm and $s = 5$ MPa. The Callister model calculates $\sigma_R = 1$ at $\phi_p > 0.006$ and $L_c > 2$ μm, while the highest σ_R of about 1.9 is obtained by $\phi_p = 0.002$ and $L_c = 1$ μm. The low relative strength at high levels of ϕ_p and L_c indicates the non-strengthening of the matrix by the addition of nanoparticles. This evidence is due to the undesirable effects of high values of ϕ_p and L_c on the yield strength of the PCNT. A high ϕ_p demonstrates the formation of the CNs network at large CNT concentrations, which means that the low fraction of CNT does not form a network and cannot significantly strengthen the polymer matrix. Furthermore, a high level of L_c indirectly indicates the poor interfacial adhesion between the polymer matrix and the CNT nanoparticles. A high L_c shows that the low surface area of the tubes can effectively transfer the stress from the polymer matrix to the nanoparticles, which produces a poor yield strength in the PCNT. According to this explanation, observing a low strength at the high levels of ϕ_p and L_c is reasonable. However, a good strength is obtained by the low levels of the ϕ_p and L_c factors in the PCNT. The small values of ϕ_p and L_c demonstrate the formation of the CNT network at low CNT concentration and an efficient stress transfer from the polymer matrix to the nanoparticles at a high region of CNT, respectively. In this condition, the CNT network forms by the low volume fraction of the nanoparticles and, also, the CNT show a high level of interfacial bonding and stress transfer. Therefore, obtaining an acceptable strength in this condition is expected.

Figure 5 also illustrates the roles of the ϕ_p and τ parameters on the yield strength of the PCNT according to Callister model (Eq. 23) at $\phi_f = 0.02$, $\sigma_m = 40$ MPa, $\sigma_f = 1.7$ GPa and $s = 5$ MPa. The ϕ_p parameter alone controls the level of strength in the PCNT based on this model. Also, the τ parameter does not change the values of σ_R. As a result, the yield strength of the PCNT mainly depends on the level of ϕ_p. In this condition, the poorest strength is calculated by $\phi_p > 0.009$ and the highest is obtained by $\phi_p = 0.002$. Thus, the ϕ_p parameter indirectly affects the σ_R in the PCNT. As mentioned, a low level of ϕ_p shows the formation of the network in the PCNT by a small amount of CNT. Therefore, the higher concentration of CNT than the percolation fraction creates a denser and stronger network in PCNT, which strengthens the PCNT more.

The τ parameter does not play a role in the yield strength of PCNT, which is similar to its effect on the modulus (Fig. 3). This occurrence is opposite to the previous findings for the effect of τ on the strength of the polymer nanocomposites, which demonstrated a direct relationship between the strength and τ as interface/interphase properties.[55,56] Possibly, the effect of the τ parameter on the strength of the PCNT is much less than that of the percolation threshold based on the Callister model. The influences of the τ factor on the mechanical behavior may change by coupling with another parameter or applying other models in this area, such as Pukanszky model. Undoubtedly, the interface/interphase parameters such as τ largely manage the level of the modulus and the strength in the PCNT, because they control the extent of stress transference between the polymer matrix and the nanoparticles.[57,58] The results in Figs. 3 and 5 indicate that the effective properties may arise from

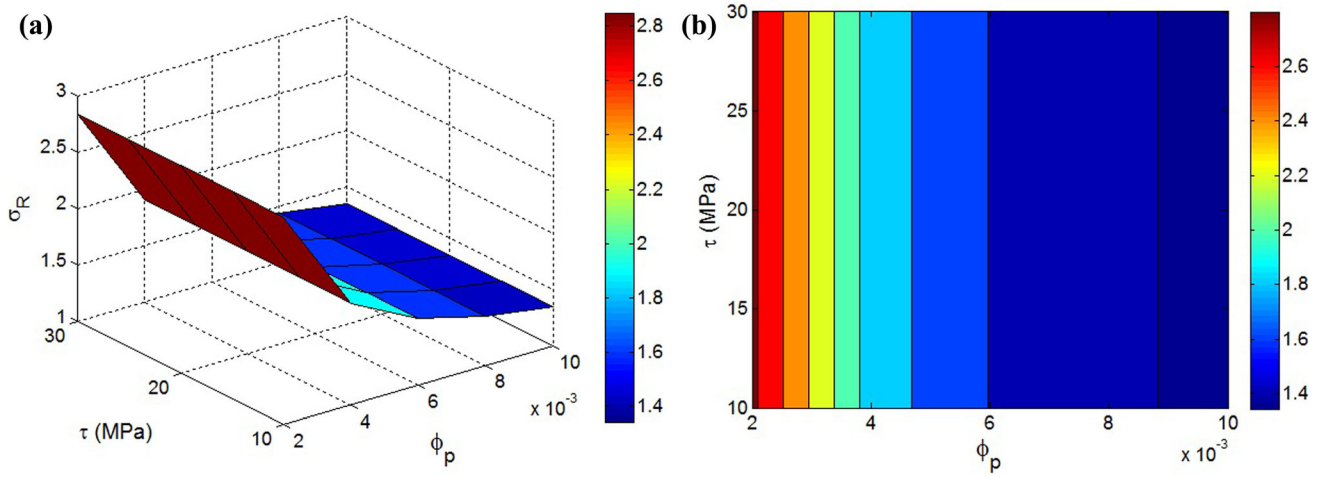

Fig. 5. The relationship between the yield strength of the PCNT and the ϕ_p and τ parameters according to the Callister model (Eq. 23) at $\phi_f = 0.02$, $\sigma_m = 40$ MPa, $\sigma_f = 1.7$ GPa and $s = 5$ MPa: (a) 3D and (b) contour plots

the consideration of extended singular chains. The lowering of the percolation threshold may increase the yield strength of the chains, as the extended chains are capable of forming above the percolation threshold.

CONCLUSION

Two known models have been applied to evaluate the effects of the filler network and imperfect interfacial adhesion on the tensile modulus and yield strength of the PCNT at the same time. The highest levels of the modulus and strength are obtained by the smallest levels of the ϕ_p and L_c parameters, while the high levels of these parameters decrease the mechanical performance. A low level of ϕ_p makes a dense and strong network of CNT in the PCNT by the low concentration of CNT, which strengthens the sample. In addition, a low L_c shows the excellent efficiency of the stress transfer between the polymer matrix and the nanoparticles in a large portion of the CNT surface, which improves the mechanical behavior. However, the ineffective role of τ as the interfacial shear strength in the mechanical performance may be due to the high level of E_f of 1000 GPa and low level of σ_f of 1.7 GPa or its smaller effect compared to the percolation threshold. Undoubtedly, the interface/interphase properties significantly affect the extent of the stress transfer between the polymer matrix and the nanoparticles managing the level of the modulus and strength in the nanocomposites.

REFERENCES

1. A. Farahi, G.D. Najafpour, and A. Ghoreyshi, *JOM* 71, 285 (2019).
2. Y. Zare and K.Y. Rhee, *JOM* 71, 3980 (2019).
3. A. Adegbenjo, P. Olubambi, J. Westraadt, M. Lesufi, and M. Mphahlele, *JOM* 71, 2262 (2019).
4. A.M. Okoro, S.S. Lephuthing, S.R. Oke, O.E. Falodun, M.A. Awotunde, and P.A. Olubambi, *JOM* 71, 567 (2019).
5. S. Arora, M. Rekha, A. Gupta, and C. Srivastava, *JOM* 70, 2590 (2018).
6. S.M. Naghib, M. Rabiee, and E. Omidinia, *Int. J. Electrochem. Sci.* 9, 2301 (2014).
7. Y. Zare and K.Y. Rhee, *Compos. Part B* 156, 100 (2019).
8. Y. Zare and K.Y. Rhee, *Polym. Compos.* 40, 4135 (2019).
9. R. Salahandish, A. Ghaffarinejad, S.M. Naghib, K. Majidzadeh-A, and A. Sanati-Nezhad, *IEEE Sens. J.* 18, 2513 (2018).
10. E. Askari and S.M. Naghib, *Int. J. Electrochem. Sci.* 13, 886 (2018).
11. A.H.Z. Kalkhoran, O. Vahidi, and S.M. Naghib, *Euro. J. Pharm. Sci.* 111, 303 (2018).
12. P.S. Bharadiya, M.K. Singh, and S. Mishra, *JOM* 71, 838 (2019).
13. B.G. Compton, N.S. Hmeidat, R.C. Pack, M.F. Heres, and J.R. Sangoro, *JOM* 70, 292 (2018).
14. S.M. Naghib, *Micro Nano Lett.* 14, 462 (2019).
15. A.K. Kasar, G. Xiong, and P.L. Menezes, *JOM* 70, 829 (2018).
16. S.M. Naghib, E. Parnian, H. Keshvari, E. Omidinia, and M. Eshghan-Malek, *Int. J. Electrochem. Sci.* 13, 1013 (2018).
17. A.H.Z. Kalkhoran, S.M. Naghib, O. Vahidi, and M. Rahmanian, *Biomed. Phys. Eng. Express* 4, 055017 (2018).
18. X. Tian, Y. Hu, J. Zhang, X. Guo, R. Bai, and L. Zhao, *J. Mater. Sci.* 54, 14975 (2019).
19. Y. Zare and K.Y. Rhee, *Compos. Part B* 175, 107132 (2019).
20. Y. Zare and K.Y. Rhee, *Compos. Part B* 161, 601 (2019).
21. Y. Zare, S.P. Park, and K.Y. Rhee, *Results Phys.* 13, 102245 (2019).
22. A. Rostami, F. Eskandari, M. Masoomi, and M. Nowrouzi, *J. Oil Gas Petrochem. Technol.* 6, 28 (2019).
23. A. Rostami, M. Vahdati, and H. Nazockdast, *Polym. Compos.* 39, 2356 (2018).
24. R. Razavi, Y. Zare, and K.Y. Rhee, *Polym. Compos.* 40, 801 (2019).
25. M. Jomaa, L. Roiban, D. Dhungana, J. Xiao, J. Cavaillé, L. Seveyrat, L. Lebrun, G. Diguet, and K. Masenelli-Varlot, *Compos. Sci. Technol.* 171, 103 (2019).
26. G. Santoro, M.A. Gomez, C. Marco, and G. Ellis, *Macromol. Mater. Eng.* 295, 652 (2010).
27. A. Alian, S. El-Borgi, and S. Meguid, *Comput. Mater. Sci.* 117, 195 (2016).
28. Y. Zare and K.Y. Rhee, *Compos. Part B* 158, 162 (2019).
29. Y. Zare and K. Rhee, *Phys. Mesomech.* 21, 351 (2018).
30. S.S.E. Bakhtiari, S. Karbasi, S.A.H. Tabrizi, and R. Ebrahimi-Kahrizsangi, *Polym. Compos.* 40, E1622 (2019).
31. S. Kim, Y. Zare, H. Garmabi, and K.Y. Rhee, *Sens. Actuators A* 274, 28 (2018).
32. C. Wan and B. Chen, *J. Mater. Chem.* 22, 3637 (2012).
33. M.M. Shokrieh and R. Rafiee, *Compos. Struct.* 92, 647 (2010).
34. Y. Zare, S. Rhim, H. Garmabi, and K.Y. Rhee, *J. Mech. Behav. Biomed. Mater.* 80, 164 (2018).
35. Y. Zare, K.Y. Rhee, and S.-J. Park, *J. Ind. Eng.* 69, 331 (2019).
36. R. Shokri-Oojghaz, R. Moradi-Dastjerdi, H. Mohammadi, and K. Behdinan, *Polym. Compos.* 40, E1918 (2019).
37. H. Daghigh and V. Daghigh, *Polym. Compos.* 40, E1479 (2019).
38. Y. Zare and K.Y. Rhee, *JOM* 71, 3989 (2019).
39. X. Ma, Y. Zare, and K.Y. Rhee, *Nanoscale Res. Lett.* 12, 621 (2017).
40. S. Gupta, R. Sachan, A. Bhaumik, and J. Narayan, *Nanotechnology* 29, 45LT02 (2018).
41. J. Narayan, S. Gupta, A. Bhaumik, R. Sachan, F. Cellini, and E. Riedo, *MRS Commun.* 8, 428 (2018).
42. S. Gupta, R. Sachan, A. Bhaumik, P. Pant, and J. Narayan, *MRS Commun.* 8, 533 (2018).
43. Y. Zare, K.Y. Rhee, and S.-J. Park, *Results Phys.* 14, 1 (2019).
44. Y. Zare and K.Y. Rhee, *J. Alloys Compd.* 793, 1 (2019).
45. J. Sandler, J. Kirk, I. Kinloch, M. Shaffer, and A. Windle, *Polymer* 44, 5893 (2003).
46. E. Garboczi, K. Snyder, J. Douglas, and M. Thorpe, *Phys. Rev. E* 52, 819 (1995).
47. V. Favier, H. Chanzy, and J. Cavaille, *Macromolecules* 28, 6365 (1995).
48. C.J. Plummer, M. Rodlert, J.-L. Bucaille, H.J. Grünbauer, and J.-A.E. Månson, *Polymer* 46, 6543 (2005).
49. X.-F. Wu and Y.A. Dzenis, *J. Appl. Phys.* 98, 093501 (2005).
50. J. Åström, J. Mäkinen, M.J. Alava, and J. Timonen, *Phys. Rev. E* 61, 5550 (2000).
51. A.P. Chatterjee, *J. Appl. Phys.* 100, 054302 (2006).
52. D. Shia, C. Hui, S. Burnside, and E. Giannelis, *Polym. Compos.* 19, 608 (1998).
53. J. Halpin and J. Kardos, *J. Appl. Phys.* 43, 2235 (1972).
54. W.D. Callister and D.G. Rethwisch, *Materials Science and Engineering: An Introduction* (New York: Wiley, 2007).
55. Y. Zare, *RSC Adv.* 6, 57969 (2016).
56. Y. Zare, *Mech. Mater.* 85, 1 (2015).
57. Y. Zhong, J. Wang, Y.M. Wu, and Z. Huang, *Compos. Sci. Technol.* 64, 1353 (2004).
58. P. Joshi and S. Upadhyay, *Comput. Mater. Sci.* 87, 267 (2014).